

A&A manuscript no.  
(will be inserted by hand later)

Your thesaurus codes are:  
11.13.1, 11.19.4

ASTRONOMY  
AND  
ASTROPHYSICS

# Morphologies and ages of star cluster pairs and multiplets in the Small Magellanic Cloud

M.R. de Oliveira<sup>1</sup>, C.M. Dutra<sup>1</sup>, E. Bica<sup>1</sup>, and H. Dottori<sup>1</sup>

Instituto de Física-UFRGS, CP 15051, CEP 91501-970 POA - RS, Brazil

Received 2 May 2000 / Accepted

**Abstract.** An isophotal atlas of 75 star cluster pairs and multiplets in the Small Magellanic Cloud is presented, comprising 176 objects. They are concentrated in the SMC main body. The isophotal contours were made from Digitized Sky Survey\* images and showed relevant structural features possibly related to interactions in about 25% of the sample. Previous N-body simulations indicate that such shapes could be due to tidal tails, bridges or common envelopes. The diameter ratio between the members of a pair is preferentially in the range 1 – 2, with a peak at 1. The projected separation is in the range  $\approx 3 - 22$  pc with a pronounced peak at  $\approx 13$  pc. For 91 objects it was possible to derive ages from Colour-Magnitude Diagrams using the OGLE-II photometric survey. The cluster multiplets in general occur in OB stellar associations and/or HII region complexes. This indicates a common origin and suggests that multiplets coalesce into pairs or single clusters in a short time scale. Pairs in the SMC appear to be mostly coeval and consequently captures are a rare phenomenon. We find evidence that star cluster pairs and multiplets may have had an important role in the dynamical history of clusters presently seen as large single objects.

**Key words:** Magellanic Clouds – Star Clusters

\*The images in this study are based on photographic data obtained using the UK Schmidt Telescope, which was operated by the Royal Observatory Edinburgh, with funding from the UK Science and Engineering Research Council, until 1988 June, and thereafter by the Anglo-Australian Observatory. Original plate material is copyright by the Royal Observatory Edinburgh and the Anglo-Australian Observatory. The plates were processed into the present compressed digital form with their permission. The Digitized Sky Survey was produced at the Space Telescope Science Institute under US Government grant NAG W-2166.

## 1. Introduction

Star cluster pairs are common objects in the Magellanic Clouds and it is important to understand their formation and evolution processes. A list of 30 cluster pairs in the SMC was first presented by Hatzidimitriou & Bhatia (1990). Bica & Schmitt (1995, hereafter BS95) revised previous data on SMC extended objects (star clusters, associations and emission nebulae) and identified new ones using Sky Survey ESO/SERC R and J films. They presented a list of 40 pairs and 2 triple star clusters. Pietrzyński & Udalski (1999a) reported 23 pairs and 4 triplets derived from Pietrzyński et al.'s (1998) star cluster catalogue in the OGLE survey area. Bica & Dutra (2000) updated BS95's catalogue considering the entries in Pietrzyński et al.'s catalogue. Bica & Dutra (2000) indicated 75 pairs and multiplets comprising 176 individual objects.

In recent years there has been growing evidence of interacting star clusters in the Magellanic Clouds, especially in the LMC. Bhatia & Hatzidimitriou (1988) concluded that more than 50% of LMC pairs must be physical systems. Bhatia & McGillivray (1988) found evidence that NGC2214 is a merging binary star cluster, based on the presence of a flattened core and an extended halo. Indeed Sagar et al. (1991) detected two turnoff points revealing the presence of two interacting clusters. Bica et al. (1992) studied cluster pairs and multiplets in the LMC bar by means of integrated colours and found systems which resulted coeval and some with age differences. Vallenari et al (1998) confirmed such scenarios by means of colour-magnitude diagrams. They also presented isophotal contours indicating physical interaction. Several other studies have found binarity evidence in LMC cluster pairs (e.g. Kontizas et al. 1993, Dieball & Grebel 2000a, 2000b).

Bhatia et al. (1991) presented a photographic atlas of binary star cluster candidates in the LMC. For the SMC no morphological atlas is available and isophotal maps are required to test possible physical interactions. Indeed comparisons of isophotes with isopleth maps of N-body simulations proved to be a useful tool (Rodrigues et al. 1994, de Oliveira et al. 1998, hereafter ODB98), since the simulations produce features such as bridges, common envelopes

and extensions. The observational importance of tidal tails as interaction signatures was also indicated by Leon et al. (1999).

In this work we provide isophotal maps for SMC pairs and multiplets to study the following properties of these candidate physical systems: (i) angular distribution; (ii) projected centre-to-centre separation of members; (iii) isophotal structures using the Digitized Sky Survey\* (hereafter DSS); (iv) ages derived by means of isochrone fitting, when possible. We discuss candidate physical systems and infer a scenario for their formation and evolution.

In Sect. 2 we gather the objects providing coordinates, sizes, centre-to-centre separations and other details for the SMC pairs and multiplets. In Sect. 3 we provide the isophotal contour atlas together with classifications of interaction features whenever present. A preliminary version of the present isophotal SMC atlas together with one for the LMC was given in de Oliveira (1996). In Sect. 4 we derive cluster ages by means of Colour-Magnitude diagrams extracted from the OGLE-II BVI photometric survey (Udalski et al. 1998). In Sect. 5 we discuss the properties of the systems and the possible scenarios for their origin and evolution. Finally, concluding remarks are given in Sect. 6.

## 2. SMC pairs and Multiplets

Table 1 shows data for the 176 SMC objects which form 75 star cluster pairs and multiplets (Bica & Dutra 2000), considering that the pair BS63/B67 in the latter study is possibly a triplet with NGC294 (ODB98). By columns: (1) object cross-identification in the different catalogues: N (Henize 1956), K (Kron 1956), L (Lindsay 1958), H (Hodge 1960), SL (Shapley & Lindsay 1963), B (Brück 1976), DEM (Davies et al. 1976), ESO (Lauberts 1982), H86- (Hodge 1986), MA (Meyssonnier & Azzopardi 1993), BS (Bica & Schmitt 1995), OGLE (Pietrzyński et al. 1998). Note that some are embedded objects, named after the corresponding HII region; (2) and (3) right ascension and declination for the epoch J2000, respectively; (4) object type following BS95: C for star cluster, NC for small HII regions with embedded star clusters, CN for clusters which show some traces of emission, A for associations, CA and/or AC for star clusters of low density and objects with intermediate properties, AN for associations which show some traces of emission and NA for HII regions with embedded associations; (5) and (6) major and minor sizes, respectively; (7) position angle of major axis ( $0^\circ = N$ ,  $90^\circ = E$ ); (8) centre-to-centre angular separation (1 arcsec = 0.28 pc assuming an absolute distance modulus  $(m-M) = 18.9$  for the SMC, Westerlund 1990). For triplets and multiplets we measured the separation between the two main members, as indicated in the corresponding object line in the table; (9) remarks:  $m6$ ,  $m5$ ,  $m4$ ,  $mT$  and  $mP$  indicate groups with six, five and four members, triplets and pairs, respectively. A running number identifies each can-

didate system. Abbreviations ‘br\*’ indicates that a bright star is present; ‘att’ means attached to. A hierarchical indication is given for objects embedded in or superimposed on larger ones: ‘in’ suggests a possible physical connection while ‘sup’ suggests a projection. There are 56 pairs, 15 triplets, 2 quadruplets, 1 quintuplet and 1 sextuplet. The quintuplet is located in the star forming region NGC395 with dimensions 25 pc x 18 pc which in turn is embedded in the HII complex SMC-DEM126 with 66 pc x 35 pc according to angular sizes in BS95. The sextuplet is mostly contained in the OB association H-A35 (Hodge 1985) with dimensions 57 pc x 47 pc. One quadruplet is located in H-A60 with 44 pc x 24 pc. Note that dimensions (columns 5 and 6) and position angle (column 7) are from Bica & Dutra (2000) and were measured on plates. The dimensions are in general larger than the isophotal sizes in the subsequent analyses.

## 3. The Isophotal Atlas

For isophotal analysis purposes we extracted digitized images of pairs and multiplets from the DSS. The plates are from the SERC Southern Sky Survey and include IIIa-J long (3600s), V band medium (1200s) and V band short (300s) exposures. The PDS pixel values correspond to photographic density measures from the original plates, and are not calibrated. The images were processed with the IRAF package at the Instituto de Física - UFRGS, applying a 2-d Gaussian filter to smooth out individual stars, producing isodensity maps.

We show the isophotal atlas of SMC star cluster pairs and multiplets in Figs. 1 throughout 7, where morphological evidence of interactions can be searched for. In each panel we point members and provide designations.

### 3.1. Isophotal Distortions

Cluster pairs and multiplets with evidence of physical interaction are marked in column 6 of Table 2. Their isophotal maps show features such as isophotal distortions, common envelope, isophotal twistings, etc. We classified these isophotal maps according to the following criteria: (i) isophotes of the members are detached (**d**), but showing isophotal distortions; (ii) isophotes of the members are connected by a “bridge” (**b**); (iii) the members are embedded in the same isophotal envelope (**e**). These classification criteria are an important tool for a selection of interacting cluster pair candidates, since such isophotal morphologies are predominant in N-body model encounters (Rodrigues et al. 1994, ODB98). The classifications above were made for objects not disturbed by gas emission. It is worth noting that both bridges and envelopes imply a common outer isophotal, however the former includes a dimension which is considerably smaller than the smaller cluster diameter. The pair B59/SMC-N46 would be an envelope limiting case (Fig. 4).

**Table 1.** SMC pairs and multiplets

Name	RA(2000) h : m : s	Dec(2000) ° : ' : "	T	Dmax "	Dmin "	PA °	Separ. "	Comments
(1)	(2)	(3)	(4)	(5)	(6)	(7)	(8)	(9)
BS3	0:30:01	-73:20:01	AC	33	33	-	31	mT-1
H86-2	0:30:04	-73:20:35	AC	39	36	80	31	mT-1
BS4	0:30:07	-73:20:58	C	33	27	70		mT-1
BS7	0:32:43	-73:37:59	C	33	33	-	59	mP-1
BS8	0:32:56	-73:38:33	AC	36	36	-		mP-1
H86-22	0:34:53	-73:02:08	C	18	18	-	42	mP-2
BS9	0:35:02	-73:02:14	AC	45	39	100		mP-2
HW9	0:36:25	-73:00:05	C	45	45	-	52	mP-3
HW10	0:36:31	-72:59:13	C	57	57	-		mP-3
B9	0:37:13	-72:57:53	C	27	27	-	68	mP-4 in H-A1
H86-41	0:37:29	-72:57:48	C	33	24	50		mP-4
H86-38	0:37:24	-73:01:50	A	72	72	-	46	mP-5
BS10	0:37:34	-73:01:30	C	39	39	-		mP-5
BS14,SMC_OGLE165	0:39:12	-73:14:46	C	33	33	-	44	mP-6
SMC_OGLE5	0:39:22	-73:15:28	CA	51	45	90		mP-6
HW12A	0:39:26	-73:22:59	C	33	27	10	36	mP-7
H86-54	0:39:35	-73:22:58	C	33	33	-		mP-7
B15	0:39:42	-72:58:39	CA	36	27	100	30	mP-8
H86-57	0:39:47	-72:58:56	CA	30	30	-		mP-8
BS13	0:40:08	-72:45:30	CA	54	45	40	48	mP-9
BS248	0:40:15	-72:46:02	AC	39	30	70		mP-9
NGC220,K18,L22,ESO29SC3	0:40:31	-73:24:10	C	72	72	-	88	mT-2,in H-A3 & SMC_OGLE8
NGC222,K19,L24,ESO29SC4	0:40:44	-73:23:00	C	72	72	-	88	mT-2,in H-A3 & SMC_OGLE9
B23,SMC_OGLE170	0:40:55	-73:24:07	C	36	30	40		mT-2,in H-A3
B19	0:40:44	-73:03:42	C	27	21	170	32	mT-3
B20	0:40:49	-73:04:09	C	18	18	-	32	mT-3
H86-62,SMC_OGLE10	0:40:48	-73:05:17	C	36	36	-		mT-3
NGC231,K20,L25,ESO29SC5	0:41:06	-73:21:07	C	108	108	-	36	mP-10,in H-A3 & SMC_OGLE11
BS15	0:41:21	-73:20:31	A	138	138	-		mP-10,in H-A3
B21,SMC_OGLE171	0:41:15	-72:49:55	C	21	21	-	34	mP-11
B22	0:41:21	-72:49:32	C	21	21	-		mP-11
B29	0:42:11	-73:43:51	CA	30	21	100	46	mP-12
HW16,SMC_OGLE13	0:42:22	-73:44:03	CN	36	36	-		mP-12,in SMC-DEM7
NGC241,K22w,L29W,	0:43:33	-73:26:25	C	57	57	-	23	mP-13 & ESO29SC6w,SMC_OGLE17
NGC242,K22e,L29e,	0:43:38	-73:26:37	C	45	45	-		mP-13 & ESO29SC6e,BH1,SMC_OGLE18
B31,SMC_OGLE19,SMC_OGLE175	0:43:38	-72:57:31	C	30	24	150		mT-4
BS20,SMC_OGLE20	0:43:38	-72:58:48	C	27	27	-	30	mT-4
H86-70,SMC_OGLE21	0:43:44	-72:58:36	C	39	27	50	30	mT-4
BS27,SMC_OGLE177	0:44:55	-73:10:27	C	24	21	80	19	mP-14,in H86-72
SMC-N10,L61-60,SMC-DEM11,	0:44:56	-73:10:11	NC	21	21	-		mP-14,in H86-72 & MA85
NGC248n,SMC-N13B,L61-67n	0:45:24	-73:22:34	NA	42	36	110	21	mP-15 & SMC-DEM16n,ESO29EN8n,MA101,SMC_OGLE26n
NGC248s,SMC-N13A,L61-67s	0:45:26	-73:23:04	NC	42	33	150		mP-15 & SMC-DEM16s,ESO29EN8s,MA103,SMC_OGLE26s
B39,SMC_OGLE27	0:45:26	-73:28:53	C	33	33	-	15	mP-16
BS30	0:45:30	-73:29:06	C	24	24	-		mP-16
B36	0:45:44	-72:50:35	C	42	36	140	10	mP-17
SMC_OGLE31	0:45:51	-72:50:25	CA	33	27	90		mP-17, not B36
B38	0:45:54	-72:36:08	C	18	18	-	38	mP-18
H86-79	0:45:58	-72:35:36	C	27	27	-		mP-18
H86-76,SMC_OGLE182	0:46:02	-73:23:44	C	27	27	-		mT-5,in SMC-DEM21
H86-78n,SMC_OGLE33n	0:46:12	-73:23:27	CN	27	27	-	16	mT-5,in SMC-N16
H86-78s,SMC_OGLE33s	0:46:12	-73:23:39	CN	27	24	60	16	mT-5,in SMC-N16
L31,SMC_OGLE36	0:46:35	-72:44:32	C	66	51	-		mT-6
H86-83,SMC_OGLE35	0:46:34	-72:46:26	C	42	42	-	30	mT-6
H86-84,SMC_OGLE185	0:46:34	-72:45:56	C	24	24	-	30	mT-6
H86-86,SMC_OGLE40	0:47:01	-73:23:35	C	48	39	110	71	mP-19,in H-A9
H86-87,SMC_OGLE187	0:47:06	-73:22:17	C	48	42	90		mP-19,in H-A9
H86-95	0:47:37	-73:00:51	CA	21	12	100	30	mP-20
H86-96	0:47:44	-73:00:46	C	18	18	-		mP-20
BS35,SMC_OGLE42	0:47:50	-73:28:42	C	42	42	-	55	mP-21
K25,L35,SMC_OGLE45	0:48:01	-73:29:10	C	72	72	-		mP-21
MA205	0:48:07	-73:14:49	NC	15	15	-	37	mT-7
SMC-N25,L61-106,SMC-DEM38,	0:48:09	-73:14:19	NA	51	51	-		mT-7 & MA208,SMC_OGLE189
SMC-N26,L61-107,MA206	0:48:08	-73:14:53	NC	27	27	-	37	mT-7
H86-99,SMC_OGLE190	0:48:13	-72:47:35	CA	39	39	-	27	mP-22
H86-100,SMC_OGLE191	0:48:20	-72:47:42	CA	45	45	-		mP-22
B50	0:49:02	-73:21:44	C	33	33	-	66	mT-8
BS41,SMC_OGLE194	0:49:06	-73:21:10	C	33	33	-		mT-8
L39,SMC_OGLE54	0:49:18	-73:22:20	C	42	33	170	66	mT-8,in BS43
SMC-N33,L61-138,MA297	0:49:29	-73:26:33	NC	18	15	80	12	mP-23,in SMC-DEM44
MA301	0:49:30	-73:26:23	NC	21	18	80		mP-23,in SMC-DEM44
SMC_OGLE56	0:49:36	-72:50:13	CA	48	36	100	70	mT-9,in SMC-DEM46e
H86-110	0:49:44	-72:51:14	CA	45	33	160	70	mT-9
H86-109,SMC_OGLE58	0:49:45	-72:51:58	C	27	27	-		mT-9
MA317	0:49:42	-73:10:37	NC	18	15	20	20	mP-24
SMC-N34,L61-142,SMC-DEM50,	0:49:46	-73:10:25	NC	39	27	120		mP-24 & MA322
B53,SMC_OGLE197	0:50:04	-73:23:04	C	57	57	-	80	mP-25
B55,SMC_OGLE60	0:50:22	-73:23:16	C	42	36	110		mP-25
SMC_OGLE199	0:50:15	-73:03:15	CA	15	15	-	35	mP-26, in? sup? SMC-DEM51
BS45,SMC_OGLE59	0:50:16	-73:02:00	CA	60	54	70		mP-26,in SMC-DEM51
H86-106w	0:50:31	-73:20:11	C	30	24	90	23	mP-27,in SMC-DEM52
H86-106e	0:50:37	-73:20:11	C	33	27	80		mP-27,in SMC-DEM52
H86-115,SMC_OGLE63	0:50:37	-73:03:28	AC	96	72	40	77	mP-28,in SMC-DEM51

Table 1. Continued.

Name	RA(2000) h : m : s	Dec(2000) ° : ' : "	T	Dmax "	Dmin "	PA °	Separ. "	Comments
(1)	(2)	(3)	(4)	(5)	(6)	(7)	(8)	(9)
SMC-N46,L61-184,SMC-DEM62,	0:51:47	-72:50:47	NC	39	39	-		mP-31 & MA498
H86-120	0:51:46	-73:28:01	C	21	21	-	43	mT-10,in SMC-DEM70s
BS53	0:51:49	-73:28:38	A	39	33	150		mT-10,in SMC-DEM70s
H86-122	0:51:58	-73:27:41	C	27	27	-	43	mT-10,in SMC-DEM70s
BS56,SMC_OGLE77	0:52:13	-73:00:12	C	42	33	90	56	mP-32
H86-130,SMC_OGLE78	0:52:17	-73:01:04	C	45	36	0		mP-32
B64,SMC_OGLE210	0:52:30	-73:02:59	C	42	42	-	56	mP-33,in H-A29
BS57,SMC_OGLE211	0:52:32	-73:02:10	C	39	27	60		mP-33,in H-A29
H86-134w,SMC_OGLE212	0:52:45	-72:59:24	C	30	30	-	19	mT-11,in H-A30
B65,SMC_OGLE83	0:52:44	-72:58:48	C	45	45	-		mT-11
H86-134e,SMC_OGLE213	0:52:48	-72:59:22	C	30	27	0	19	mT-11,in H-A30
BS61	0:52:43	-73:01:45	CA	36	27	80	42	mP-34,in H-A29
BS255	0:52:52	-73:01:45	C	24	18	70		mP-34
BS63,SMC_OGLE84	0:52:47	-73:24:25	C	30	24	150	19	mT-12,in SMC-DEM73
B67,SMC_OGLE87	0:52:49	-73:24:43	C	39	30	110		mT-12,in SMC-DEM73
NGC294,L47,ESO29SC22,	0:53:06	-73:22:49	C	102	102	-		mT-12 & SMC_OGLE90
H86-140,SMC_OGLE214	0:53:09	-72:49:58	C	27	24	50	15	mP-35
H86-139	0:53:11	-72:50:05	C	21	18	40		mP-35
BS67	0:53:32	-73:21:03	AC	39	39	-	51	mP-36
BS68,SMC_OGLE95	0:53:42	-73:21:32	CA	54	45	130		mP-36
B72	0:53:26	-72:40:57	C	72	72	-		m6,in H-A35
H86-143,SMC_OGLE93	0:53:31	-72:40:04	C	48	48	-		m6,in H-A35
BS257	0:53:36	-72:38:30	AC	48	39	0		m6
SMC-N52A,L61-243,	0:53:40	-72:39:35	NC	30	30	-	20	m6,in H-A35 & SMC-DEM77sw,MA696,SMC_OGLE94
SMC-N52B,L61-244,B73,	0:53:42	-72:39:15	NC	30	30	-	20	m6,in H-A35 & SMC-DEM77ne,MA699,SMC_OGLE96
H86-148	0:53:55	-72:40:08	C	30	30	-		m6,in H-A35
BS69,SMC_OGLE217	0:53:56	-72:51:24	CA	36	24	45	75	mP-37
BS72,SMC_OGLE97	0:54:11	-72:51:54	CA	45	36	20		mP-37
B78	0:54:45	-72:07:46	C	66	48	110	56	mP-38,in H-A37
L51,ESO51SC7	0:54:54	-72:06:46	C	60	45	170		mP-38,in H-A37
H86-159,SMC_OGLE102	0:55:12	-72:41:00	C	30	24	130	45	mP-39,in BS260
H86-160	0:55:21	-72:40:10	C	24	24	-		mP-39,in BS260
BS81,SMC_OGLE223	0:56:26	-72:29:45	C	36	33	0	43	mP-40,in H-A40
H86-172,SMC_OGLE108	0:56:34	-72:30:08	C	33	33	-		mP-40,in H-A40
H86-175,SMC_OGLE227	0:57:50	-72:26:24	C	24	24	-	38	mP-41
H86-179,SMC_OGLE112	0:57:57	-72:26:42	C	24	24	-		mP-41
H86-177,SMC_OGLE226	0:57:50	-72:30:29	C	45	45	-	46	mP-42,in B-OB13
H86-176	0:57:53	-72:29:48	C	36	30	90		mP-42
SMC-N62,SMC-DEM93	0:57:56	-72:39:26	NA	72	72	-	75	mT-13,in H-A42
SMC-N63,L61-331,SMC-DEM94,	0:58:16	-72:38:47	NA	36	36	-		mT-13,in H-A42 & MA1065,SMC_OGLE113
SMC-N64A,L61-335,SMC-DEM95	0:58:26	-72:39:57	NC	48	39	70	75	mT-13,in SMC-N64 & H86-182,MA1071,SMC_OGLE114
BS269	0:58:19	-72:13:10	CA	24	18	60	35	mP-43
BS270	0:58:23	-72:12:43	CA	33	30	130		mP-43
BS271	0:58:37	-72:13:27	NC	39	30	30	35	mP-44,in SMC-DEM98
BS272,SMC_OGLE229	0:58:38	-72:14:04	NC	39	39	-		mP-44,in SMC-DEM98
BS93	0:59:36	-71:44:13	C	24	21	10	17	mT-14,in SMC-DEM105
B97	0:59:37	-71:44:40	C	30	30	-		mT-14,in SMC-DEM105
BS273	0:59:40	-71:44:34	AC	30	27	120	17	mT-14,in SMC-DEM105
IC1611,K40,L61,ESO29SC27,	0:59:48	-72:20:02	C	90	90	-		m4-1 & SMC_OGLE118
H86-186,SMC_OGLE119	0:59:57	-72:22:24	C	36	36	-	29	m4-1,att SMC-DEM114
IC1612,K41,L62,ESO29SC28,	1:00:01	-72:22:08	C	72	48	20	29	m4-1,att SMC-DEM114 & SMC_OGLE120
K42,L63,SMC_OGLE124	1:00:34	-72:21:56	C	51	51	-		m4-1,att SMC-DEM114
B98sw	1:00:21	-73:52:51	C	36	27	40	33	mP-45
B98ne	1:00:28	-73:52:32	C	33	27	130		mP-45
H86-189,SMC_OGLE123	1:00:33	-72:14:23	C	24	24	-	68	mP-46
H86-190,SMC_OGLE230	1:00:33	-72:15:31	C	24	24	-		mP-46
H86-191,SMC_OGLE231	1:00:58	-72:32:25	C	48	48	-	81	mP-47,in? SMC-DEM114
H86-194,SMC_OGLE232	1:01:14	-72:33:03	C	51	51	-		mP-47,in? SMC-DEM114
BS102	1:01:14	-73:47:45	C	30	21	100	42	mP-48
HW44	1:01:22	-73:47:15	C	45	45	-		mP-48
B110	1:02:11	-72:00:11	C	33	27	70	65	mP-49, br*in,in H-A49
B112	1:02:23	-72:00:11	C	51	45	60		mP-49, br*in,in H-A49
K45w,L69w	1:02:45	-73:44:19	C	33	27	40	47	mP-50
K45e,L69w	1:02:49	-73:44:25	C	24	24	-		mP-50
NGC376,K49,L72,ESO29SC29,	1:03:53	-72:49:34	C	108	108	-	75	mP-51 & SMC_OGLE139
BS114,SMC_OGLE235	1:03:59	-72:48:18	AC	42	30	110		mP-51
SMC_OGLE138	1:03:53	-72:06:11	CA	36	36	-	82	mP-52,in H-A53
SMC_OGLE144,SMC_OGLE236	1:04:05	-72:07:15	CA	36	36	-		mP-52
BS122	1:04:18	-73:10:21	C	21	21	-	26	mP-53
B119	1:04:19	-73:09:54	C	36	36	-		mP-53
SMC-N78A,L61-438,MA1512	1:05:04	-71:59:01	NC	24	21	140	23	m5,in NGC395
SMC-N78B,L61-439,	1:05:04	-71:59:25	NC	24	18	100		m5,in NGC395 & MA1508/1514,SMC_OGLE145
MA1520,SMC_OGLE147	1:05:08	-71:59:45	NC	30	27	130	23	m5,in NGC395
SMC-N78D,SMC-DEM127	1:05:11	-71:58:28	NA	54	54	-		m5,att SMC-N78
SMC_OGLE146	1:05:13	-71 59 42	NA	27	27	-		m5,in NGC395
BS130	1:05:56	-72:04:11	A	57	36	140	30	mP-54,att SMC-N78
BS132	1:06:01	-72:03:37	CA	42	33	150		mP-54,att SMC-N78
BS133	1:06:23	-71:55:12	A	39	30	30		mT-15,in BS134
BS135	1:06:40	-71:55:13	CA	39	39	-	47	mT-15,in BS134
BS136	1:06:48	-71:54:55	CA	42	42	-	47	mT-15,in SMC-DEM132
B134	1:09:01	-73:12:24	CA	48	33	80		m4-2,in H-A60
BS142	1:09:07	-73:12:01	C	24	21	70	31	m4-2,in H-A60
IC1644,SMC-N81,L61-481,	1:09:13	-73:11:43	NC	48	39	40	31	m4-2,in H-A60 & ESO29EN25,MA1688/1687

As examples, the pair H86-186/IC1612 (Fig. 5) is embedded in the same isophotal envelope and it is classified as **e**. The pair H86-140/H86-139 (Fig. 4) shows a bridge linking its members and is classified as **b**. In Fig. 6 the pair NGC376/BS114 shows isophotal distortions, however the outer isophotes of the components are not connected and it is thus classified as **d**.

We detected relevant isophotal features for about 25% of the sample distributed as follows: 6 candidate cluster systems with common envelope, 7 with bridge and 5 detached cases.

High isophotal densities such as those observed for B78/L51 (Fig. 5) are related to the high surface brightness which often occurs in blue clusters.

It is important to note that non relevant isophotal features can appear in the maps caused by bright stars or background fluctuations. By means of previous inspections in the original images we verified the non relevant objects. For example, the compact object in the lower right corner of the B39/BS30 isophotal map (Fig. 2) is a bright star, however the compact one to the right of the main cluster can be a star or a compact cluster, as seen in the original form. Higher resolution images would be necessary to check the presence of a third cluster.

#### 4. Ages of cluster members

Udalski et al. (1998) provided a BVI photometric survey of the SMC central  $\approx 2.4$  square degrees with results for about 2.2 million stars. The data were collected during the OGLE-II microlensing search project (Udalski et al. 1997).

Pietrzyński & Udalski (1999b) studied colour-magnitude diagrams (CMDs) extracted from the BVI database for 93 SMC star clusters, taking into account neighbouring field extractions for comparisons. They estimated reddening values for each cluster using: (i) the mean I band magnitude of red clump stars in the cluster neighbourhood; (ii) the assumed extinction-free magnitude of the SMC's red clump stars,  $I = 18.34$  mag (Udalski 1998). They derived ages using Bertelli et al.'s (1994) isochrones, adopting as a rule for the SMC a metallicity  $Z = 0.004$ , and an absolute distance modulus  $(m-M) = 18.65$ .

Considering the OGLE-II angular coverage we conclude that out of the present 176 objects 133 are therein included. We obtained from the database V and I band CMDs for these objects, using their coordinates and diameters to define a box extraction. Guided by DSS images of each system we selected representative field regions to extract stars and construct CMDs for comparison purposes. Ages and reddenings for the clusters were estimated by fitting the Padova isochrones. We adopted Bertelli et al.'s (1994) isochrones rather than the new isochrones by Girardi et al. (2000), since the previous set includes younger ages. The isochrone age grid suitable for 4, 5, 6.3, 7.9, 10, 12, 16, 20, 25, 32, 40, 50, 63, 79, 100, 126, 160, 199, 251,

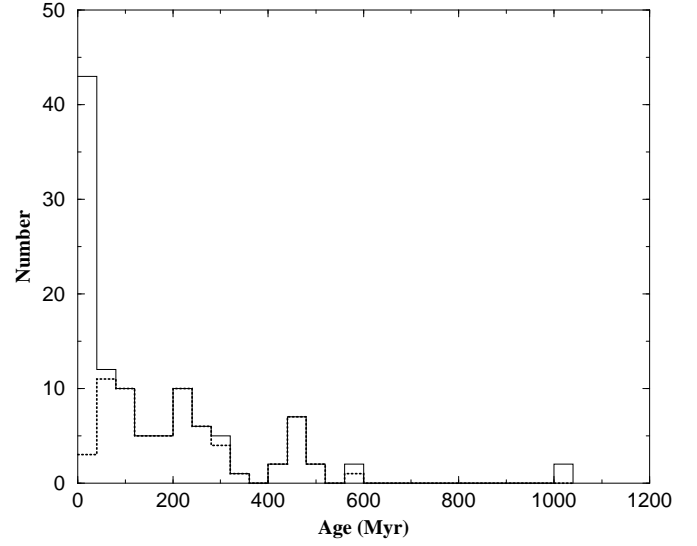


**Fig. 8.** Age histograms: dotted lines represent clusters with age via CMDs; solid lines are for the same sample as above plus embedded clusters in HII regions, assuming an age 3 Myr. In the latter histogram lower or upper limits in Table 2 were also included by adopting them as cluster ages.

316, 400, 500, 630, 790 and 1000 Myr. The isochrone age range and resolution allow one to estimate errors taking into account the stellar statistics in the cluster and field CMDs. We also assumed a SMC metallicity of  $Z = 0.004$ , a foreground galactic reddening of  $E(B-V)_f = 0.03$  in the SMC direction and  $E(V-I)/E(B-V) = 1.31$ . Table 2 shows the ages, in column 2 and reddening values (foreground plus SMC internal) in column 3 determined in the present work via isochrone fitting. Ages and reddening values derived by Pietrzyński & Udalski (1999b) are in column 4 and 5 respectively, when available for comparisons. In our sample we could estimate CMD ages for 91 objects, 40 of them in common with Pietrzyński & Udalski (1999b). We conclude that despite the reddening method and distance modulus differences between the two studies, there is good overall agreement for the age determinations. We also included ages for 21 objects embedded in HII regions, classified as NA and NC (see column 4 of Table 1, and also BS95). We assumed for them an age of 3 Myr.

#### 5. Discussion

We overlap two age histograms in Fig. 8. The dotted line histogram shows objects from Table 2 with ages via CMDs. There are three peaks, at about 80, 220 and 450 Myr. The first two peaks appear to be present in Grebel et al.'s (2000) sample for 200 SMC clusters based on OGLE-II data, reported at  $t \approx 100$  and 200 Myr respectively. They suggested them as enhanced star formation epochs. Considering Pietrzyński & Udalski's (1999b) sample with CMD ages for 93 SMC clusters, no peak is seen at  $t =$

**Table 2.** Age, Reddening and Morphological Classification

Name	Age Myr	E(B-V)	Age <sub>OGLE</sub> Myr	E(B-V) <sub>OGLE</sub>	Morphologies	Comments
(1)	(2)	(3)	(4)	(5)	(6)	(7)
BS3					b	mT-1 outside OGLEII
H86-2					b	mT-1 outside OGLEII
BS4						mT-1 outside OGLEII
H86-38	251±25	0.10				mP-5
BS10	>560	0.10				mP-5
B15	>1000	0.07				mP-8
H86-57	>1000	0.07				mP-8
NGC220,SMC_OGLE8	65±13	0.07	100±23	0.07	d	mT-2
NGC222,SMC_OGLE9	70±7	0.07	100±23	0.07	d	mT-2
B23,SMC_OGLE170	<100	0.07			d	mT-2
NGC231,SMC_OGLE11	65±8	0.12	79±18	0.08		mP-10
BS15	70±7	0.10				mP-10
B29	150±70	0.10				mP-12
HW16,SMC_OGLE13	<20	0.07	20±15	0.05		mP-12
NGC241,SMC_OGLE17	55±5	0.12	79±18	0.10	b	mP-13
NGC242,SMC_OGLE18	65±10	0.10	79±18	0.10	b	mP-13
B31,SMC_OGLE19,SMC_OGLE175	280±30	0.10	400±92	0.08		mT-4
BS20,SMC_OGLE20	450±50	0.08	400±92	0.08		mT-4
H86-70,SMC_OGLE21	450±50	0.07				mT-4
BS27,SMC_OGLE177	<25	0.18	79±37	0.08		mP-14
SMC-N10	HII Region					mP-14
NGC248n,SMC_OGLE26n	HII Region					mP-15
NGC248s,SMC_OGLE26s	HII Region					mP-15
B39,SMC_OGLE27	450±50	0.07			b	mP-16
BS30	450±50	0.07			b	mP-16
B36	315±50	0.03				mP-17
SMC_OGLE31	450±50	0.03				mP-17
H86-76,SMC_OGLE182	200±20	0.14				mT-5
H86-78n,SMC_OGLE33n	<25	0.14	16±9	0.15		mT-5
H86-78s,SMC_OGLE33s	<30	0.14	16±9	0.15		mT-5
L31,SMC_OGLE36	250±50	0.10				mT-6
H86-83,SMC_OGLE35	180±50	0.10				mT-6
H86-84,SMC_OGLE185	250±50	0.10				mT-6
H86-86,SMC_OGLE40	350±50	0.03				mP-19
H86-87,SMC_OGLE187	140±20	0.07	158±36	0.04		mP-19
BS35,SMC_OGLE42	400±100	0.03				mP-21
K25,SMC_OGLE45	250±50	0.07	250±58	0.07		mP-21
MA205	HII Region				b	mT-7
SMC-N25,SMC_OGLE189	HII Region				b	mT-7
SMC-N26	HII Region					mT-7
H86-99,SMC_OGLE190	225±50	0.14			d	mP-22
H86-100,SMC_OGLE191	200±50	0.14			d	mP-22
B50	<30	0.10				mT-8
BS41,SMC_OGLE194	70±30	0.10	79±18	0.07		mT-8
L39,SMC_OGLE54	80±20	0.10	100±23	0.10		mT-8
SMC-N33	HII Region				e	mP-23
MA301	HII Region				e	mP-23
SMC_OGLE56	115±15	0.18				mT-9
H86-110	<20	0.18				mT-9
H86-109,SMC_OGLE58	180±20	0.18	200±45	0.17		mT-9
MA317	HII Region				b	mP-24
SMC-N34	HII Region				b	mP-24
B53,SMC_OGLE197	200±50	0.07	250±55	0.08		mP-25
B55,SMC_OGLE60	160±30	0.07	250±55	0.08		mP-25
SMC_OGLE199	—	—				mP-26
BS45,SMC_OGLE59	65±30	0.10	63±14	0.10		mP-26
H86-106w	200±50	0.10			e	mP-27
H86-106e	<30/200±50 <sup>1</sup>	0.12/0.10			e	mP-27
H86-115,SMC_OGLE63	—	—				mP-28
SMC_OGLE65	200±20	0.10				mP-28
BS46,SMC_OGLE200	80±10	0.07	100±23	0.06	b	mP-29
H86-116,SMC_OGLE64	125±15	0.10	126±29	0.10	b	mP-29
BS48,SMC_OGLE201	160±20	0.10				mP-30
H86-108,MA401	<30	0.12				mP-30
B59,SMC_OGLE73	100±15	0.14	158±75	0.11	e	mP-31
SMC-N46	HII Region				e	mP-31

**Fig. 1.** Isophotal atlas of SMC cluster pairs and multiplets.**Fig. 2.** Isophotal atlas of SMC cluster pairs and multiplets.**Fig. 3.** Isophotal atlas of SMC cluster pairs and multiplets.

**Table 2.** Continued.

Name	Age Myr	E(B-V)	Age <sub>OGLE</sub> Myr	E(B-V) <sub>OGLE</sub>	Morphologies	Comments
(1)	(2)	(3)	(4)	(5)	(6)	(7)
BS56,SMC_OGLE77	140±20	0.07	79±38	0.08	d	mP-32
H86-130,SMC_OGLE78	65±8	0.12	79±18	0.08	d	mP-32
B64,SMC_OGLE210	<10	0.12	158±75	0.07	d	mP-33
BS57,SMC_OGLE211	<10	0.12				mP-33
H86-134w,SMC_OGLE212	—	—				mT-11
B65,SMC_OGLE83	65±10	0.10	63±30	0.09		mT-11
H86-134e,SMC_OGLE213	—	—				mT-11
BS61	250±50	0.03				mP-34
BS255	—	—				mP-34
BS63,SMC_OGLE84	450±50	0.10			d	mT-12
B67,SMC_OGLE87	450±50	0.10	500±115	0.10	d	mT-12
NGC294,SMC_OGLE90	300±50	0.10	316±73	0.11	d	mT-12
H86-140,SMC_OGLE214	55±25	0.10			b	mP-35
H86-139	<30	0.10			b	mP-35
BS67	>300	0.07				mP-36
BS68,SMC_OGLE95	500±100	0.07				mP-36
B72	80±10	0.10				m6
H86-143,SMC_OGLE93	200±25	0.10				m6
BS257	50±30 <sup>1</sup>	0.10				m6
SMC-N52A,SMC_OGLE94	HII Region					m6
SMC-N52B,SMC_OGLE96	HII Region					m6
H86-148	400±100	0.10				m6
H86-159,SMC_OGLE102	500±50	0.10				mP-39
H86-160	—	—				mP-39
BS81,SMC_OGLE223	80±20/250±50 <sup>1</sup>	0.10				mP-40
H86-172,SMC_OGLE108	280±30	0.07				mP-40
H86-175,SMC_OGLE227	30±10	0.10				mP-41
H86-179,SMC_OGLE112	<30	0.10	32±23	0.11		mP-41
H86-177,SMC_OGLE226	<30	0.10			d	mP-42
H86-176	<30	0.10			d	mP-42
SMC-N62	HII Region					mT-13
SMC-N63,SMC_OGLE113	HII Region					mT-13
SMC-N64A,SMC_OGLE114	HII Region					mT-13
BS269	—	—				mP-43
BS270	<30	0.10				mP-43
BS271	<30	0.12				mP-44
BS272,SMC_OGLE229	<30	0.08	79±18	0.05		mP-44
IC1611,SMC_OGLE118	100±20	0.07	160±37	0.08		m4-1
H86-186,SMC_OGLE119	180±20	0.07			e	m4-1
IC1612,SMC_OGLE120	100±50	0.10	50±24	0.07	e	m4-1
K42,SMC_OGLE124	20±10	0.10	40±9	0.06		m4-1
H86-189,SMC_OGLE123	570±70	0.07				mP-46
H86-190,SMC_OGLE230	125±13	0.07	32±23	0.08		mP-46
H86-191,SMC_OGLE231	200±25	0.07				mP-47
H86-194,SMC_OGLE232	200±25	0.07				mP-47
NGC376,SMC_OGLE139	20±2	0.10	32±7	0.07	e	mP-51
BS114,SMC_OGLE235	250±25	0.04			e	mP-51
SMC_OGLE138	<30	0.04	25±20	0.04		mP-52
SMC_OGLE144,SMC_OGLE236	<30	0.07	40±19	0.05		mP-52
SMC-N78A	HII Region					m5
SMC-N78B,SMC_OGLE145	HII Region		79±37	0.07		m5
MA1520,SMC_OGLE147	HII Region		12±9	0.06		m5
SMC-N78D	HII Region					m5
SMC_OGLE146	HII Region		20±15	0.06		m5
BS130	80±10	0.10				mP-54
BS132	<30/200±25 <sup>1,2</sup>	0.10				mP-54
HW71nw					e	mP-56 outside OGLEII
HW71se					e	mP-56 outside OGLEII

Notes to Table 2: 1- Age depends on membership of bright stars; 2- Upper main sequence is possibly underpopulated.

**Fig. 4.** Isophotal atlas of SMC cluster pairs and multiplets.

**Fig. 5.** Isophotal atlas of SMC cluster pairs and multiplets.

**Fig. 6.** Isophotal atlas of SMC cluster pairs and multiplets.

**Fig. 7.** Isophotal atlas of SMC cluster pairs and multiplets.

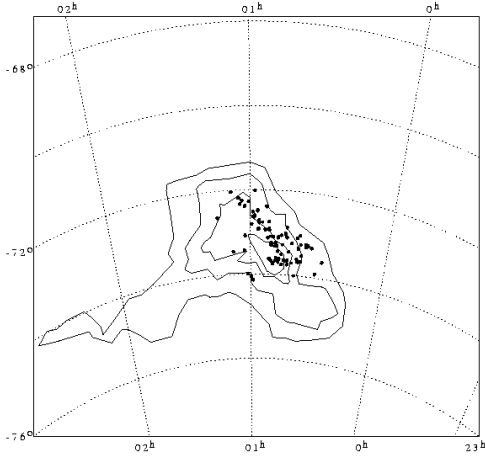


**Fig. 9.** Angular distribution of the 176 objects in SMC cluster pairs and multiplets together with HI contours 100, 200, 400 and 600 in units  $10^{19}$  atoms  $cm^{-2}$  from Mathewson & Ford (1984).

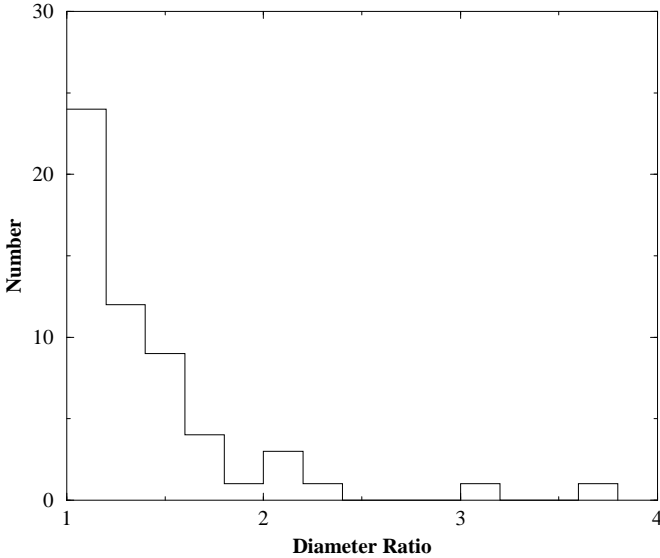


**Fig. 10.** The observed diameter ratio distribution for SMC cluster pairs

80-100 Myr, having their histogram a maximum at the youngest bin. In their histogram there occurs a local maximum at  $t \approx 250$ -300 Myr, but the statistics is low. The third peak in the present study has no counterpart in both previous analyses, and it is probably an artifact from the low isochrone age step resolution in that range.

The solid line histogram in Fig. 8 shows additionally the embedded objects in HII regions for which we assumed an age of 3 Myr, and the objects from Table 2 with lower or upper limits by assuming them as the ages themselves. We can observe again a three peak distribution but the first peak is now shifted to the youngest bin similarly to

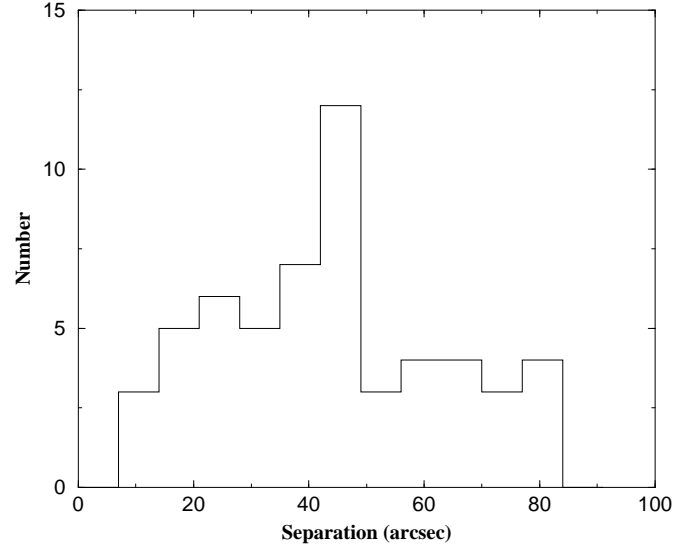


**Fig. 11.** Centre-to-centre angular separation distribution for SMC cluster pairs

Pietrzyński & Udalski's (1999b) histogram. This suggests that only the 200 Myr peak is relevant, being related to the SMC/LMC last encounter (Gardiner et al. 1994, Grebel et al.'s 2000). The maximum seen in the youngest bin is possibly related to the cluster formation/destruction rates. Since the present sample deals with pairs and multiplets a fast destruction rate might be caused by the internal dynamical evolution in each cluster complex, caused by merger and/or other effects.

Approximately 55% of cluster pairs and multiplets in Table 2 present similar ages between their members indicating that they are coeval. This suggests that most of the pairs and multiplets had a common origin, possibly from the same molecular complex. Note that about 60% of the pairs and multiplets embedded in OB associations (H-A, Hodge 1985), as indicated in column 9 of Table 1, have comparable ages between their members. This could be an explanation for the origin of cluster systems.

Considering triplet and multiplet members, we found that about 70% of them are younger than 100 Myr. These results suggest a possible binary cluster formation scenario: clusters can be born in multiplet systems and coalesce by mergers and tidal disruptions forming binary clusters in a timescale of  $\approx 100$  Myr. This time is in agreement with dynamical times required for an interacting pair to merge into a single cluster (ODB98, de Oliveira et al. 2000).

The pairs with a bridge in the isophotal maps have comparable ages for their components (Table 2). As examples, the pairs NGC241/NGC242 and B39/BS30 in Fig. 2 show a bridge linking their members which could be interpreted as a sign of interaction (see the similarity with the N-body simulation model in Fig. 11 of ODB98). A typical timescale for the bridge phenomenon is  $\approx 30$  Myr,



as deduced from a series of N-body simulations related to bridge formation and evolution (ODB98).

Another interesting isophotal feature is related to the cluster triplet NGC220/NGC222/B23 which shows distortions for the small cluster in a direction almost perpendicular to the line connecting itself to the large components NGC220 and NGC222. This configuration and morphologies are compatible with a fast hyperbolic encounter with small impact parameter (e.g. Fig. 12 of ODB98).

Fig. 9 shows the angular distribution of pairs and multiplets together with SMC HI column density isophotes from Mathewson & Ford (1984). It can be seen that most of the objects are concentrated in the SMC main body, close to the higher concentration of HI, so it is not unexpected that in general they result young (Sect. 4). The objects appear to be distributed along an axis. Such distribution is present in the overall SMC cluster sample and there is growing evidence that it is related to a nearly edge-on disk containing the bulk of the young stellar population in the SMC (Bica *et al.* 1999, Westerlund 1990).

A nearly edge-on disk in a low internal reddening galaxy like the SMC would imply an increase of projection effects as compared to a simulation such as that carried out by Bhatia & Hatzidimitriou (1988) for the nearly face-on LMC disk where the physical pairs would be about 50%. Consequently the fraction of physical pairs in the SMC would be lower. The present approach including morphological evidence of interaction is an attempt to constrain this aspect. Indeed the fraction with isophotal distortions is only 25% (Sect. 3.1). Projection effects can be responsible for the age spread in some multiplets. For example the sextuplet (Table 2) has component ages 80 Myr (B72), 200 Myr (H86-143), 50 Myr (BS257), 3 Myr (SMC-N52A and SMC-N52B) and 400 Myr (H86-148). Possibly only the 3 or 4 younger components could be related to OB-Association H-A35, the remaining objects would be captures or projection effects. This age spread is also present in IC1611's quadruplet and in some triplets. On the other hand the quintuplet in the star forming complex NGC395 has all its members with the same age (3 Myr) thus forming a physical system.

In Fig. 10 we show the distribution of the diameter ratio between members for all pairs in the sample. The diameter ratio is mostly in the range 1 – 2, with a peak at 1 indicating that the majority of pair members have a comparable size. This effect was also observed in the LMC (Bhatia *et al.* 1991).

Fig. 11 shows the distribution of the centre-to-centre angular separation between pair members. The separation range is  $\approx 10 - 80$  arcsec ( $\approx 3 - 22$  pc) with a pronounced peak at  $\approx 45$  arcsec (13 pc). A similar peak was also observed by Bhatia *et al.* (1991) and de Oliveira (1996) who found a bimodal distribution for the LMC pairs with peaks at  $\approx 5$  and 13 pc. The observed upper limit of the projected centre-to-centre linear separation  $\approx 23$  pc (80 arcsec) is comparable to Bhatia & Hatzidimitriou's (1988)

separation criterion for pairs in the LMC (18.7 pc). The frequent separation value around 13 pc may reflect a preferred survival distance for the systems, combined to projection effects.

## 6. Conclusions

We presented an isophotal atlas for 75 star cluster pairs and multiplets in the Small Magellanic Cloud, comprising 176 objects.

It was possible to derive ages from Colour-Magnitude Diagrams using the OGLE-II photometric survey for 91 objects. In addition we included in the analysis ages for 21 embedded objects in HII regions. The age distribution has a maximum in the youngest bin with a profile related to the cluster formation/destruction rates, in particular cluster multiple systems can have a fast destruction rate caused by their internal dynamical evolution. There is a second peak around 220 Myr which is probably related to the SMC/LMC last encounter.

We find that 55% of the pairs and multiplets in the sample are in general coeval, indicating that captures are a rare phenomenon. Most of the cluster multiplets occur in OB stellar associations and/or HII region complexes which indicates a common origin and suggests that multiplets coalesce into pairs or single clusters in a short time scale ( $\approx 100$  Myr).

The majority of the cluster members have comparable sizes, with a diameter ratio ranging mostly between 1 – 2. The projected separation distribution between the members of a pair has a pronounced peak at  $\approx 13$  pc. These observational results are important constraints to theoretical models of star cluster pair encounters and could be related with the formation process and subsequent dynamical evolution of cluster systems.

The angular distribution of cluster pairs and multiplets shows that most of the objects are located in the SMC main body. The overall SMC cluster sample presents a similar distribution and there is evidence that it is related to a nearly edge-on disk in the SMC. Considering this, it is expected an increase of projection effects as compared to estimates for the LMC disk where physical pairs would be about 50% (Bhatia & Hatzidimitriou 1988).

The atlas shows that around 25% of the isophote maps present relevant structures like bridges, common envelopes or detached distorted isophotes. N-body simulations have indicated that these structures arise from interactions between the members of the cluster systems. Indeed cluster pairs as NGC241/NGC242 and B39/BS30 show in their isophotal maps bridges linking their members and have comparable ages.

We conclude that multiplicity may have an important role in the early dynamical evolution of star clusters in general, and signatures of that may survive in the long term structure of large single clusters (de Oliveira *et al.* 2000).

*Acknowledgements.* We thank the referee Dr. B. Westerlund for interesting remarks. We acknowledge support from the Brazilian institutions CNPq, CAPES and FINEP.

## References

- Bertelli G., Bressan A., Chiosi C., 1994. *A&AS*, 106, 275.
- Bhatia R.K., Hatzidimitriou D., 1988. *MNRAS*, 230, 215.
- Bhatia R.K., MacGillivray H.T., 1988. *A&A*, 203, L5.
- Bhatia R.K., Read M.A., Hatzidimitriou D., Tritton S., 1991. *A&AS*, 87, 335.
- Bica E., Schmitt H., 1995. *ApJS*, 54, 33.
- Bica E., Clariá J.J., Dottori H., 1992. *AJ*, 103, 1859.
- Bica E., Dutra C.M., 2000. *AJ*, 119, 1214.
- Bica E., Schmitt H., Dutra C.M., Luz Oliveira H., 1999. *AJ*, 117, 238.
- Brück M., 1976. *Occas. Rep. R. Obs. Edinburgh*, 1, 1.
- Davies R.D., Elliot K.H., Meaburn S., 1976. *MNRAS*, 81, 89.
- de Oliveira M.R., 1996. *MSc Thesis, Universidade Federal do Rio Grande do Sul, Porto Alegre*.
- de Oliveira M.R., Dottori H., Bica E., 1998. *MNRAS*, 295, 921.
- de Oliveira M.R., Bica E., Dottori H., 2000. *MNRAS*, 311, 589.
- Dieball A., Grebel E.K., 2000a. *A&A*, in press, astro-ph0004208.
- Dieball A., Grebel E.K., Theis C., 2000b. *A&A*, in press, astro-ph0004119.
- Gardiner L.T., Sawa T., Fujimoto M., 1994. *MNRAS*, 266, 567.
- Girardi L., Bressan A., Bertelli G., Chiosi C., 2000. *A&AS*, 141, 371.
- Grebel E.K., Zaritsky D., Harris J., 2000. in *News Views of the Magellanic Clouds. In: Proceedings of the IAU Symp. 190*, eds. You-Hua Chu, Nicholas B. Suntzeef, James E. Hesser, David A. Bohlender (eds)., *PASP Conf. Series*, p. 405.
- Hatzidimitriou D., Bhatia R.K., 1990. *A&A*, 230, 11.
- Henize K., 1956. *ApJS*, 12, 163.
- Hodge P.W., 1960. *ApJ*, 131, 351.
- Hodge P.W., 1985. *PASP*, 97, 530.
- Hodge P.W., 1986. *PASP*, 98, 1113.
- Kontizas E., Kontizas M., Michalitsianos A., 1993. *A&A*, 267, 59.
- Kron G.E., 1956. *PASP*, 68, 125.
- Lauberts A., 1982. *The ESO/Uppsala Survey of the ESO (B) Atlas*, Munich:ESO.
- Leon S., Bergond G., Vallenari A., 1999. *A&A*, 344, 450.
- Lindsay E.M., 1958. *MNRAS*, 118, 172.
- Mathewson D.S., Ford V.L., 1984. *Structure and Evolution of the Magellanic Clouds. In: Proceedings of the IAU Symp. 108*, S.van den Bergh, K.de Boer (eds). Kluwer, Dordrecht.
- Meyssonier N., Azzopardi M., 1993. *A&AS*, 102, 451.
- Pietrzyński G., Udalski A., 1999a. *Acta Astron*, 49, 165.
- Pietrzyński G., Udalski A., 1999b. *Acta Astron*, 49, 157.
- Pietrzyński G., Udalski A., Szymański et al., 1998. *Acta Astron*, 48, 175.
- Rodrigues I., Rodriguez A., Schmitt H., Dottori H., Bica E., 1994. *Proceedings of the IIIrd ESO/CTIO Workshop on The Local Group: Comparative and Global Properties*, A.Layden, R.C.Smith, J.Storm.
- Sagar R., Richtler T., de Boer K.S., 1991. *A&A*, 249, L5.
- Shapley H., Lindsay E.M., 1963. *Ir. Astron. J.*, 6, 74.
- Udalski A., 1998. *Acta Astron*, 48, 383.
- Udalski A., Kubiak M., Szymański M., 1997. *Acta Astron*, 47, 319.
- Udalski A., Szymański M., Kubiak et al., 1998. *Acta Astron*, 48, 147.
- Vallenari A., Bettoni D., Chiosi C., 1998. *A&A*, 331, 506.
- Westerlund B.E., 1990. *A&AR*, 2, 29.

This figure "catal\_1.gif" is available in "gif" format from:

<http://arxiv.org/ps/astro-ph/0006369v1>

This figure "catal\_2.gif" is available in "gif" format from:

<http://arxiv.org/ps/astro-ph/0006369v1>

This figure "catal\_3.gif" is available in "gif" format from:

<http://arxiv.org/ps/astro-ph/0006369v1>

This figure "catal\_4.gif" is available in "gif" format from:

<http://arxiv.org/ps/astro-ph/0006369v1>

This figure "catal\_5.gif" is available in "gif" format from:

<http://arxiv.org/ps/astro-ph/0006369v1>

This figure "catal\_6.gif" is available in "gif" format from:

<http://arxiv.org/ps/astro-ph/0006369v1>



This figure "catal\_7.gif" is available in "gif" format from:

<http://arxiv.org/ps/astro-ph/0006369v1>